FES JOULE MILESTONE 2008
3RD QUARTER

Annual Target

Conduct experiments on major fusion facilities leading toward the predictive capability for burning plasmas and configuration optimization. In FY08, FES will evaluate the generation of plasma rotation and momentum transport, and assess the impact of plasma rotation on stability and confinement. Alcator C-Mod will investigate rotation without external momentum input, NSTX will examine very high rotation speeds, and DIII-D will vary rotation speeds with neutral beams. *The results achieved at the major facilities will provide important new data for estimating the magnitude of and assessing the impact of rotation on ITER plasmas.*

QUARTER 3 MILESTONE

With experiments in progress in all three facilities, make an initial evaluation of the results to date and adjust plans as necessary.

COMPLETION OF 3RD QUARTER MILESTONE

The 3rd Quarter FY08 JOULE Milestone target has been successfully completed. All three facilities continued with productive experiments. The experimental plan spreadsheet has been amended to show these 3rd Quarter experiments. An initial evaluation shows that there are several areas of cross-machine synergy. A majority of the experiments on the original plan have received time, and nearly all are projected to receive machine time by the end of the FY. A relatively small level of plan adjustment has taken place, largely to take advantage of emerging opportunities.

NSTX greatly improved experimental conditions with respect to minimization of magnetohydrodynamic (MHD) instabilities by a) using lithium evaporation for wall conditioning and b) improved error field correction and active mode control techniques. To take advantage of this improved performance some 2nd Quarter Joule related experiments were re-addressed.

The DIII-D results in the 2nd and 3rd Quarters have led to some plan adjustment in order to address ITER issues and opportunities in the 4th Quarter. Discretionary experimental time has been added to conduct an experiment on rotational screening or amplification of applied resonant magnetic perturbations for ELM control, in response to the ITER STAC. A similar experiment was on the spreadsheet list (exp # 21) but now has been refocused to specifically address the ITER issues. Secondly, a non-JOULE experiment in the 3rd Quarter indicated a possible path to achieve the quiescent H-mode (QH) with co-rotation, and with low rotation. A day has been added to explore this opportunity (added exp #42). Next, an experiment has been added to specifically measure the neutral beam injected (NBI) torque profile since knowledge of the input torque is very important in analysis of other experiments, such as those on modulated momentum transport (added exp #43). And lastly an experimental mini-campaign has been expanded to investigate hydrogen plasmas, as opposed to the standard deuterium, also in response to ITER needs. This provides an opportunity to measure intrinsic rotation in these H discharges to compare and contrast with our D, and He, database (added exp #44). The one DIII-D experimental area that will not receive time this run period is intrinsic rotation and momentum confinement in helium plasmas (# 25). Helium allows the ability to measure the main ion velocity, as opposed to an impurity marker ion.

The spreadsheet has been amended to also indicate those experiments that have been added and those from the original plan that will not receive run time this year.

Some areas of cross-machine synergy that have emerged in the results to date are as follows:

1. NTV experiments in NSTX and DIII-D.
2. Hollow intrinsic rotation profiles with co-LHCD in C-Mod, and former observations of hollow profiles in DIII-D ECH H-modes.
3. Extension of the C-Mod, Rice scaling, for intrinsic rotation to higher β_N in DIII-D using balanced NBI.
4. Modulated momentum transport experiments in DIII-D and NSTX with NBI and in C-Mod with rapid shape change.
5. RWM feedback stabilization in NSTX and DIII-D.
6. NTM stability dependence upon rotation in NSTX and DIII-D.

Facility Examples

C-Mod

C-Mod successfully closed out their planned run year and moved into their scheduled down time for machine inspection. A number of sessions were conducted in support of

the JOULE milestone and supporting data were obtained in other experiments. Of these specific JOULE experiments, six were newly addressed in the 3rd Quarter. There is a variety of interesting, novel, and in some cases first-measured results.

One example from C-Mod is a measurement of toroidal velocity due to mode conversion flow drive (MCFD). Mode conversion of fast waves launched from an antenna at the wall of the tokamak vessel into shorter wavelength ion waves within the plasma is being explored as a tool to generate local current drive, and plasma flow. The layer at which the mode conversion takes place is spatially localized. C-Mod has measured a very large co-I_p toroidal flow velocity in a mode conversion (MC) experiment. Some data are shown in Fig. 1. In the left panels is a comparison of a MC heating scenario with the ion cyclotron minority resonance heating (ICRH) more generally used in C-Mod. MC generates a much larger toroidal velocity, V_{tor}, than ICRH. Here $V_{\text{tor}} > 0$ is in the co-I_p direction. While the densities are matched in the two discharges there is some difference in the stored energy, W_p, and the electron and ion temperatures, T_e and T_i, respectively. These differences are no doubt due to the details of the heating mechanisms. The right panel shows the scaling of the MCFD velocity with $\Delta W_p / I_p$ (red circles) in comparison with the standard Rice scaling (asterisks), where I_p is the plasma current. MCFD is roughly a factor of two more effective than ICRH in terms of the Rice scaling parameter, which characterizes the H-mode intrinsic rotation in many tokamaks.

Concomitant with the strong toroidal rotation, a poloidal flow, V_θ, in the ion diamagnetic direction is observed in the MCFD plasma. A significant flow appears in the region of $0.3 < r/a < 0.5$, and peaks at ~ 2 km/s (~ 0.7 km/s per MW of RF power).

Momentum transport in L-mode plasmas has been investigated by taking advantage of the significant difference in plasma flows depending on the X-point location under certain operating conditions. Utilizing fast (10 ms) switching of the X-point location, which changes edge plasma rotation, and measuring the core rotation velocity profile evolution, momentum transport coefficients may be characterized. An example of this technique is demonstrated in Fig. 2, where in the left panel is shown the fast SSEP sweep [negative for lower single null (LSN) and positive for upper single null (USN)] and the response of the central rotation velocity. The SSEP parameter is a measure of the balance between upper and lower X-points. In the right panel is the rotation velocity profile evolution at several radial locations, showing the velocity perturbation propagating from the edge plasma into the core. A momentum confinement time of about 40 ms, similar to the energy confinement time, is found, which is anomalously short compared to neo-classical values. The similarity of momentum confinement and energy confinement times has been observed on many devices and thus further validates this rapid shape change method as a tool for momentum transport studies.

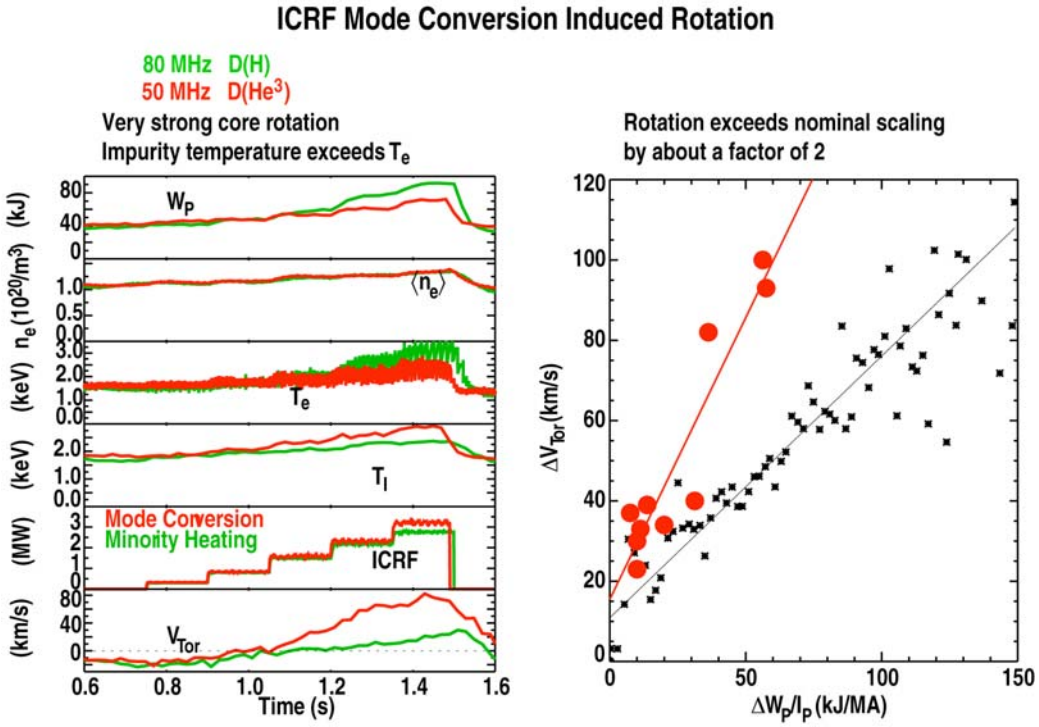

Fig. 1. (Left panels) Intrinsic toroidal velocity, V_{tor}, in a C-Mod mode conversion (MC) heated discharge (red) as compared with ion cyclotron minority resonance heating (green). (Right panel) Scaling of MC V_{tor} with $\Delta W_p / I_p$ (red circles) compared with that for ICRH (asterisks).

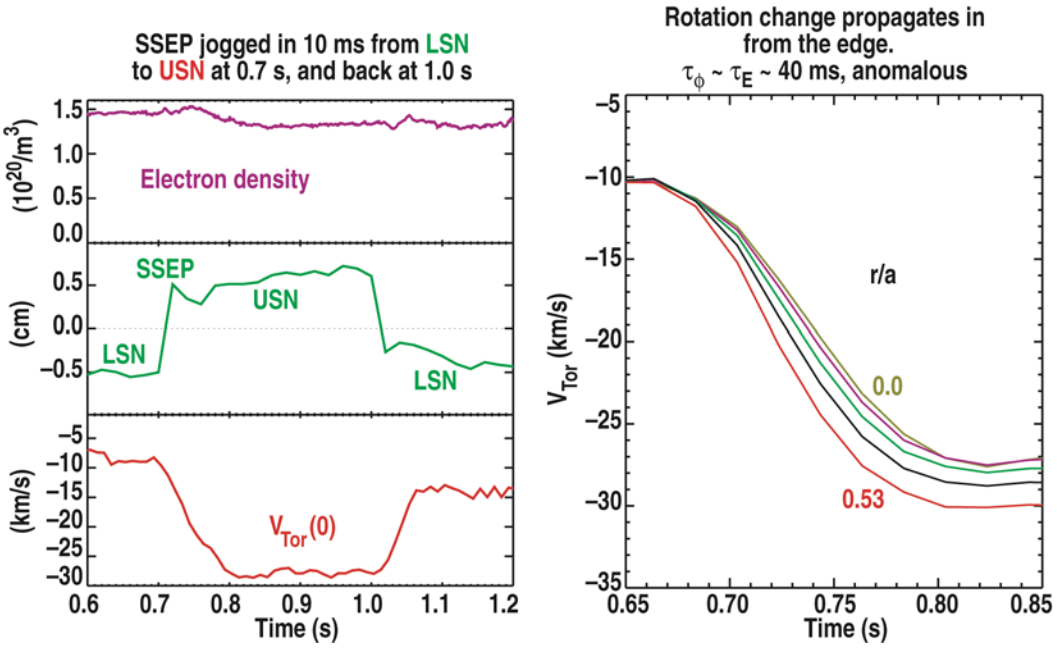

Fig. 2. L-mode momentum transport in C-Mod following fast SSEP sweeps.

NSTX

Since the FY08 2nd Quarter JOULE target report, two major operational changes were made in NSTX. The first is the use of lithium evaporation, and the second is the routine use of both $n = 3$ error field correction and $n = 1$ active mode control during the course of the entire discharge. These techniques have led to discharges that were much more reproducible and MHD-free. Typical discharges using these methods last for over 1 s, with a period of over 500 msec free of major rotating MHD modes. These changes have led to rotational changes that will aid in our understanding related results in both the transport and stability areas. In the latter area, the rotational changes appear to have profound effects on both ELM and NTM stability; these effects are under investigation and will be reported in the 4th Quarter.

During the 3rd Quarter, the decision was made to provide additional experimental time XPs 812 (Effect of rotation on energy confinement), 813 (Momentum transport using $n = 3$ braking) and 820 (Core momentum transport). When these experiments were conducted during the 2nd Quarter, the discharges contained a significant amount of low-n MHD activity that limited the discharge duration. Consequently, there were limitations on the results from the experiments in terms of the role of internal MHD magnetic perturbations vs. that of rotation in determining the discharge evolution and characteristics. These experiments were redone using the reduced-MHD discharges as baselines. The three experiments were performed over the course of 1+ days with these reproducible discharges, and full datasets for all three experiments were obtained.

Some data traces from the energy confinement experiment (XP 812) are shown in Fig. 3. Magnetic braking with an $n = 3$ perturbation was used to slow the plasma and assess the impact of rotation on confinement. The optimum $n = 3$ error correction (RWM current) is applied at $t = 250$ ms (upper panel) and is changed at 500 ms to various levels to introduce an error field. The steady-state velocity varies from 80 km/s down to 25 km/s with varying error field, as shown in the second panel. The equilibrium-determined plasma stored energy shows very little change over this range of rotation values (third panel). TRANSP analysis runs have been done for these plasmas, and the local changes in transport coefficients, rotation and rotation shear will be assessed.

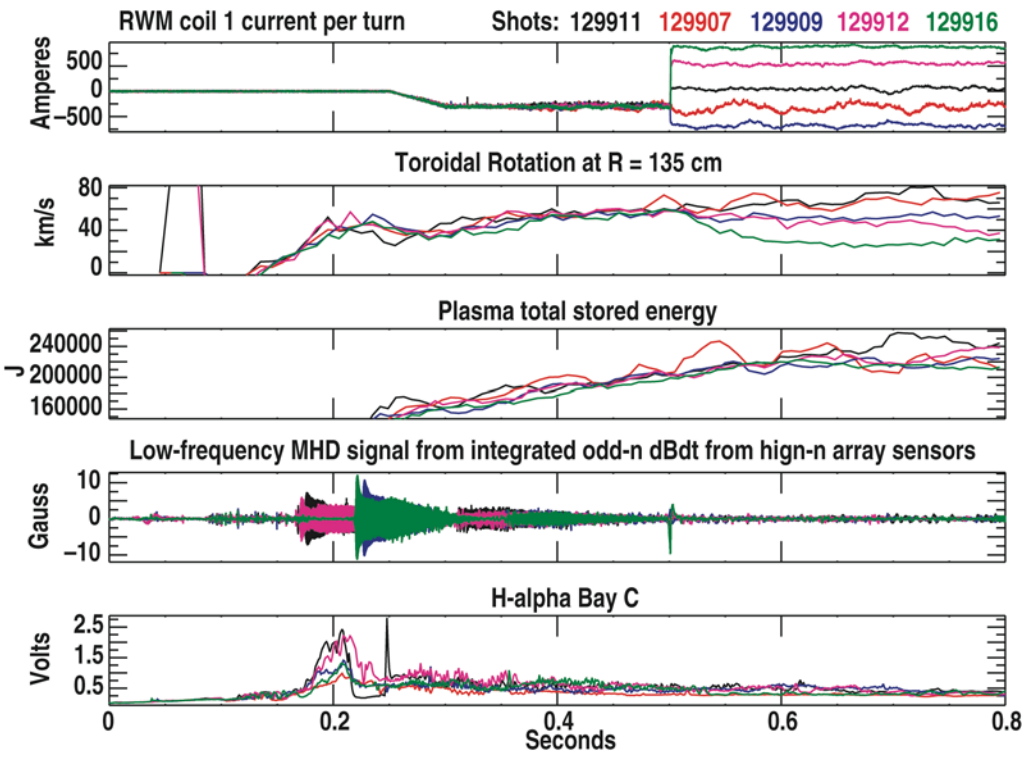

Fig. 3. Series of NSTX discharges showing varying levels of rotation near $R = 135$ cm (second panel from top). There is little change in the total stored energy (lower panel). Note the suppressed zero in the stored energy panel.

The other two re-addressed experiments cited above investigated momentum transport by utilizing pulsed magnetic $n = 3$ perturbations (XP813), similar to the energy confinement experiment above, and by utilizing torque perturbations (XP820) achieved by pulsing various neutral beam combinations. Many tokamak experiments indicate that the momentum transport is described by a diffusive process, proportional to the velocity gradient, dV_ϕ/dr, and a convective process, proportional to the velocity itself, V_ϕ. In order to separate these processes experimentally the perturbation must drive a difference in these two terms. If they are always proportional, the equations for the two transport channels cannot be solved to determine each separately. This separation was successfully achieved experimentally and example data are shown from the $n = 3$ perturbation experiment in Fig. 4. Each panel is for V_ϕ at a different major radius, R, showing the cycle followed throughout a perturbation in V_ϕ versus dV_ϕ/dr. Separability is seen roughly by the area within the paths.

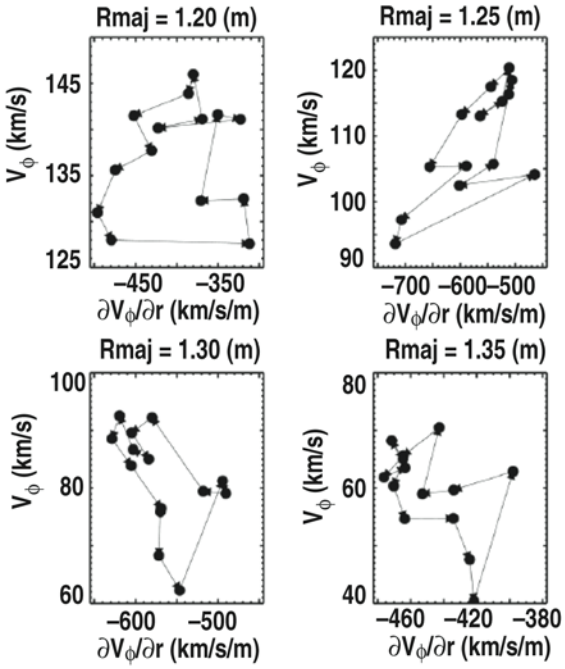

Fig. 4. Decoupling of v_ϕ and dV_ϕ/dr from the $n = 3$ braking experiment on NSTX, allowing separation of momentum diffusivity and momentum pinch.

DIII-D

DIII-D conducted many experiments dedicated to the JOULE experimental plan in the 3rd Quarter and other experiments contributed to the JOULE roster. Highlighted in Fig. 5 are sample results from an experiment to use torque-balanced neutral beam injected (NBI) heating to raise the plasma normalized energy, β_N, to higher values than achievable with rf heating alone and test the Rice scaling, i.e. velocity $\sim W/I_p$, at ITER-relevant values. In the H-mode discharge shown the NBI torque is scanned between positive (co-I_p) and negative (counter-I_p) values, as shown in Fig. 5(b). This is a control room estimate of the torque deposited in the interior of the plasma, within minor radius $\rho < 0.8$ or so. When this value is near, or slightly below zero we believe that within this minor radius there is little net torque, as indicated by the circled values. In Fig. 5(a) we show the measured toroidal velocity, V_{tor}, at $\rho \sim 0.8$ divided by W/I_p. In spite of zero net torque inside, and an excess counter torque expected outside this location, the velocity is in the co-I_p direction, demonstrating the continued intrinsic rotation at an ITER-relevant β_N value ~ 2, as shown in Fig. 5(b). The velocity scaled to W/I_p is lower than the value found in rf H-modes in DIII-D. Detailed analyses with TRANSP must be done to unfold the NBI torque profile and the plasma momentum response to see if there is actually any lingering excess counter torque that is reducing the velocity. Another possibility is that with higher heating power than available in rf H-modes the well-known power degradation of energy, and presumably momentum confinement, has reduced the velocity. The second time slice in Fig. 5 is after ECH power has been added,

resulting in a reduction in the plasma density, for as yet an unknown reason. But this serves to give us a comparison at lower density but very similar β_N.

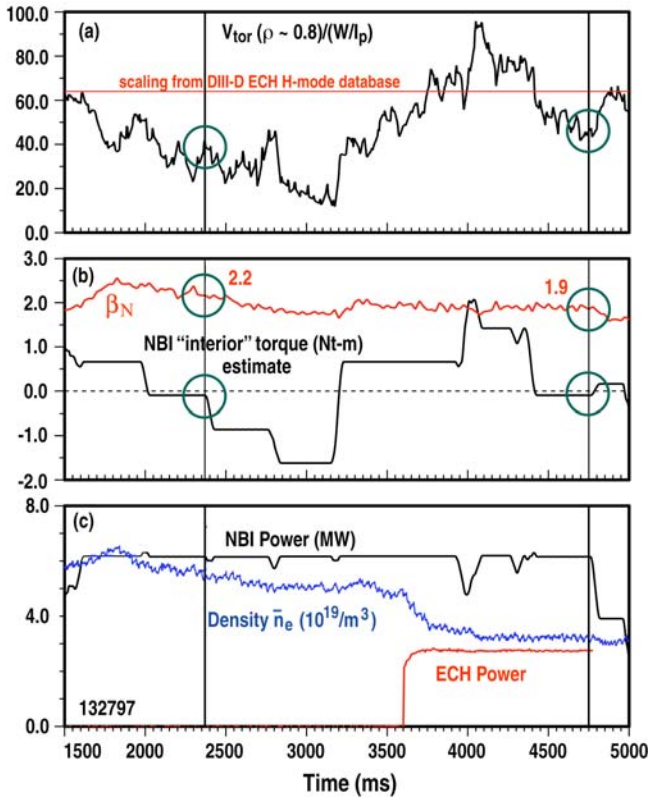

Fig. 5. Intrinsic toroidal velocity, V_{tor}, in DIII-D with balanced NBI torque injection to raise the plasma normalized stored energy, β_N, to ITER relevant values. (a) $V_{tor}/\left(W/I_p\right)$, and scaling for rf H-mode database (red line). (b) β_N and estimate of total NBI torque deposited in $\rho < 0.8$. (c) NBI power, ECH power, and line-averaged electron density.

Another experiment in DIII-D addressed the effect of toroidal rotation on the instability threshold of the NTM, as a function of β_N. High energy, β_N, leads to instability, while high co-I_p toroidal velocity is observed to have a stabilizing effect. To understand the physics, scalability and potential for control of this mode, experiments were extended to strong counter-I_p injection (where beams inject in the opposite direction to the plasma current). The results show that torque per se, or plasma rotation, is not simply stabilizing to tearing modes – with increasing counter torque, the limit first falls further before recovering somewhat. Data are plotted in Fig. 6, where the NTM stability threshold in β_N is plotted versus the NBI torque applied. Positive torque is co-I_p and leads to the highest values of β_N before the NTM instability occurs. The implications of these observations on NTM thresholds in ITER is uncertain at present. While ITER will operate with very limited torque input, the intrinsic rotation as predicted by the Rice Scaling will be quite large in ITER. Hence, the exact dependence on the NTM on torque and/or rotation is important. The observed behavior of the NTM

threshold favors a model in which sheared rotation modifies the tearing mode structure and stability, adding to, or canceling, a similar effect arising from the magnetic shear. This suggests that increases in the pressure limit might be achievable by further manipulation of the current profile.

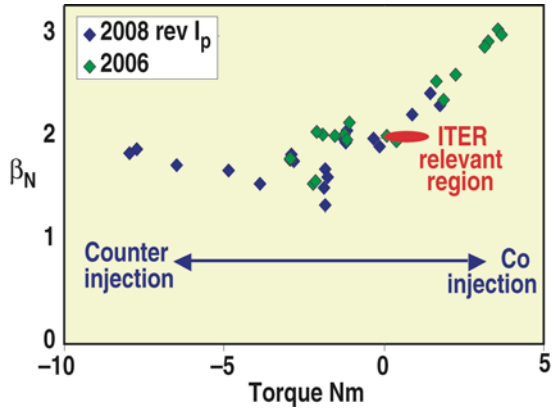

Fig. 6. Preliminary results (data to be validated) showing the trend in the 2/1 NTM pressure limit, in β_N, as torque injection to the plasma is varied for an ITER baseline-like plasma in DIII-D.

Further experiments have explored this NTM threshold sensitivity to error fields in order to provide a basis for revised error field correction requirements at low torque and intermediate β_N, relevant to the ITER baseline. These show an increased sensitivity to error field as the threshold for the $m = 2/n = 1$ NTM is approached by either torque or a β_N. Thus error field correction is more important at low torque and/or high β_N.

Websites for further information are found at:

C-Mod: List of experimental mini proposals (MPs) and links to run date where applicable.
https://www.psfc.mit.edu/research/alcator/program/cmod_runs.php?miniproposals&sort=date_filed&dir=desc

NSTX: List of experimental plans (XPs) with files that describe the XPs listed here.
http://nstx.pppl.gov/DragNDrop/XP_Folder/Approved_XPs/FY08/

DIII-D: List of experiments by date with a link to the mini proposals describing the experiments. The experimental number used in the attached spreadsheet is comprised of the numbers in columns 4 and 5.
https://diii-d.gat.com/diii-d/Expsched08

Not in priority order

FY2008 Joule Milestone 2nd Quarter Progress
C=C-Mod N=NSTX D=DIII-D

Numbers for linkages to others

Area		exp	Title	links	exp	Q2 exps	Q3 exps
IA Sources: Intrinsic	C	1	Intrinsic rotation database continuation	5,6	1	Multiple exps	Multiple exps
	C	2	Intrinsic rotation profile evolution	5,13,14	2	Multiple exps	Multiple exps
	C	3	Rotation in LHCD plasmas, (and possibly MCEH plasmas)	6	3	MP523	MP523 MP497
	C	4	Rotation inversion vs ne, Ip - in limiter/divertor plasmas		4		MP535a
	D	5	Intrinsic rotation at high normalized pressure using balanced NBI	1,2	5	02-03	02-03
	D	6	Expand DIII-D intrinsic rotation database, especially shape effects, SOL flows	1,3	6		02-06
	D	7	Measure edge turbulent momentum transport (relates to boundary condition)	8	7		02-06
	D	44	Measure intrinsic rotation in bulk ion Hydrogen discharges.	1,6	44		
	N	8	Mean and oscillating turbulent flows using Doppler reflectometry	7	8		
IB Sources: Driven	D	9	Measure off-axis NBCD and validate NBCD physics		9	55-02	55-01
	D	10	Affect of Alfven Eigenmodes on NBCD and fast ion profile†		10		57-01
	D	43	NBI torque profile	9,11	43		02-09
II Momentum Transport	N	11	Perturbative modulation of core rotation using beam blips; diffusion and pinch.	14,2	11	XP820	XP820+
	N	12	Non-core perturbative modulation of rotation using n=1 magnetic braking blips	19,20	12	XP813	XP813+
	C	13	Momentum transport, locked/unlocked	2,20,22,12	13		MP550
	C	2	Intrinsic rotation profile evolution	11,14	2		Multiple exps
	D	14	NBI modulated transport at low rotation with balanced NBI (piggybacks)	2	14		
	C	42	Momentum impulse due to rapid shape change (SSEP)	2,20,22	42	MP537	MP537
IIIA Sinks: non-resonant Δb	N	15	Comparison of NTV among tokamaks	18	15	XP804	XP804
	N	16	Island-induced NTV		16		
	D	17	Test Two vs. One row ELM-suppression coils for ITER, n=3		17	03-01	
	D	18	Test NTV offset rotation, and collisionality effect, with applied n=3	15,21	18	02-01 02-02 02-07	02-12
IIIB Sinks: resonant Δb	C	19	Intrinsic rotation with n=1 braking	12	19	MP478	MP550
	D	20	Resonant n=1 braking and error field thresholds	12,13	20	02-05	
IV Δb Penetration	D	21	RMP screening or amplification dependence upon rotation	18	21		
	C	22	Rotation in H-modes and locked modes	13	22		MP550
V Boundary Condition	C	23	Er well spatial structure and parameter scaling		23	MP538	MPs 531/32/38
	D	7	Measure edge turbulent momentum transport	8	7		02-06
	D	5-7	included in these experiments		5-7		
VI Main ion rotation/ Neoclassical theory	C	24	Edge ion rotation in helium plasmas (related to boundar condition)	25	24	MP519	
	D	25	Main ion rotation studies (helium)	24,26	25		defer
	N	26	Poloidal rotation studies; relation to neoclassical theory	25	26		
VIIA Rotation and Stability - RWM	D	27	Measure RWM damping by plasma rotation	29	27		14-03
	D	28	Demonstrate RWM feedback stabilization at low rotation		28	14-01	
	N	29	RWM stabilization and damping	27	29	XP805	XP805 XP830
	N	30	Active RWM feedback stabilization optimization		30		XP802
VIIB Rotation and Stability - NTM	N	31	Rotation dependence of 2/1 NTM thresholds	33	31	XP801 XP810	XP801 XP810
	N	32	Studies of the 3/2 NTM; rotation and rampdown	34	32		
	D	33	Effect of rotation on NTM beta limits	31	33		02-08
	D	34	NTM 3/2 mode stability at low rotation	32	34		02-08

FY2008 Joule Milestone 2nd Quarter Progress
C=C-Mod N=NSTX D=DIII-D

Not in priority order

Numbers for linkages to others

VIII Impact of Rotation on Confinement	N	35	Dependence of energy and impurity transport upon rotation (n=3 modification)		35	XP812	XP812+
	D	36	Changes in confinement with rotation		36		53-02
	C	37	Rotation during sawteeth	33	37	MP520	
IX Other Rotation Effects that impact ITER	D	38	Dependence of the L->H power threshold upon rotation		38	53-01	
	D	39	QH mode at low small plasma rotation		39	03-02	
	N	40	Dependence of the L->H power threshold upon rotation through n=3 braking		40		
	C	1	Intrinsic rotation database continuation		1		
	D	41	Effect of Core Rotation on SOL flows		41	56-01	
	D	42	QH mode in co-rotating plasmas	39	42		03-10